Institute of Experimental Morphology, Pathology and Anthropology with Museum
Bulgarian Anatomical Society

Acta Morphologica et Anthropologica, 33 (1-2)
Sofia ● 2026

Garré's Sclerosing Osteomyelitis of the Tibia in a Male from Nor Armavir (6th–5th centuries BC), Armenia

Anahit Yu. Khudaverdyan[1], Margar S. Hmayakyan[1], Shota A. Vardanyan[2], Vardan V. Margaryan[3], Nvart G. Tiratsyan[1], Anna P. Antonyan[3], Yurii M. Cherepennikov[3], Vahan R. Kocharyan[3], Simon G. Hmayakyan[1]

[1]*Institute of Archaeology and Ethnography, National Academy of Science, Yerevan, Republic of Armenia*
[2]*Department of Forensic Medicine, Yerevan Mkhitar Heratsi State Medical University, Yerevan, Republic of Armenia*
[3]*Institute of Applied Problems of Physics of National Academy of Science, Republic of Armenia*

*Corresponding author e-mail: ankhudaverdyan@gmail.com

At the Nor Armavir site, dated to the Late Iron Age, skeletal remains of adult male, aged 40–45 years, showing pathological alterations of the lower leg, were recovered. Macroscopic analysis was utilized to estimate sex and age, followed by a paleopathological differential diagnosis. Three-dimensional computed microtomography and analysis of bone microelement composition were performed to conduct a detailed examination of the tibia and to assess pathological versus post-depositional changes, thereby supporting the differential diagnosis. Our study suggests the presence of Garre's sclerosing osteomyelitis. This disease could have caused abnormal Sc content. The diagnosis of Garre's sclerosing osteomyelitis is supported by the presence of pronounced cortical thickening of the tibial diaphysis, concentric periosteal bone apposition, narrowing of the medullary cavity, and the absence of sequestra or cloacae, as demonstrated by macroscopic examination and 3D microtomographic analysis. This represents the first documented case identified among ancient inhabitants of Armenia.

Key words: Armenia, Late Iron Age, 3D computed microtomography, Garre's sclerosing osteomyelitis, scandium (Sc)

Introduction

Osteomyelitis is an inflammatory process of bone tissue that develops in response to infection, usually of bacterial origin [20]. It arises under the influence of various pathogenic microorganisms and spreads within the bone tissue. In this condition,

inflammatory bone remodeling characterized by concurrent osteolytic and osteosclerotic processes occurs, with the degree of each process depending on the virulence of the pathogenic microorganisms and the reactivity of the host organism. The most common causative agent is *Staphylococcus aureus*; less frequently, hemolytic streptococci, *Streptococcus albus*, pneumococci, *Bact. pyocyaneus*, typhoid and paratyphoid bacilli, and other pathogens are involved [27].

Osteomyelitic lesions may originate in the surrounding soft tissues, the periosteum enveloping the bone, or the bone marrow, which occupies the medullary cavity of long tubular bones as well as the spaces and sinuses between trabeculae and lamellae of the osseous tissue. Cases of osteomyelitis originating from the periosteum are relatively benign, with a slower clinical course and without extensive bone destruction. In contrast, lesions arising from the bone marrow are characterized by a more aggressive course and are associated with substantial destruction of bone tissue [30].

In 1893, the Swiss surgeon Carl Garré first provided a detailed description of ten clinical variants of acute osteomyelitis. One of these was characterized by aseptic osteosclerosis accompanied by thickening of the bone and periosteum [5, 25]. Garré's sclerosing osteomyelitis is a rare and specific form of chronic osteomyelitis, characterized by cortical thickening and obliteration of the medullary canal [32]. It predominantly affects children and young individuals [5, 12], although cases involving individuals aged 50 years and older have also been reported [35]. The scientific literature indicates that the disease primarily affects the mandible and only rarely involves the metaphysis of long bones [32], whereas other studies report a predominance of lesions in the diaphysis of the tibia (approximately 70% of cases) and the femur (27.5%) [34]. To date, the precise etiology of this condition remains unclear [5, 35].

This disorder is more frequently discussed in the dental literature, where the mandible is reported as the most commonly affected bone [12]. It is known that the chronic process may be maintained by a persistent, low-grade infection and may persist even after treatment; therefore, the role of bacterial infection in the development of this condition has not been conclusively established [5, 26]. Isotope scans may reveal increased uptake of radiotracers at the affected site [32]. Garré's osteomyelitis most frequently affects males [34, 35]. The predominant morphological feature of this rare chronic condition is fusiform thickening of the cortical layer of the affected bone. The disease is usually confined to a single bone, although multiple regions of the same bone may be involved.

The present study provides anthropological data for an individual recovered from a 6^{th}–5^{th} century BC burial at the Nor Armavir cemetery. The village of Nor Armavir is located northwest of the "Fortress of Saint David." The aim of this study is to present a detailed description of a case of tibial osteomyelitis identified in an individual from the Nor Armavir site (Armenia), to conduct a differential diagnosis, and to assess other possible conditions that may produce symptoms similar to those observed in this study.

Material and Methods

The investigation of the archaeological site of Nor Armavir (Argishtikhinili) is associated with the establishment of the capital of Greater Armenia, Armavir, in the eastern citadel of the city in the 4th century BC. Argishtikhinili is located in the Armavir Province of the Republic of Armenia. The city was founded on two hills in 776 BC by King Argishti I. Both hills – Armavir and the so-called "Fortress (or Hill) of Saint David" – have remained places of worship up to the present day. The city is mentioned in Urartian cuneiform inscriptions dating to the 8th century BC and was later described in detail in the 5th century AD by Movses Khorenatsi [17].

An important role in the early investigation of Armavir was played by the learned monks of Echmiadzin, who repeatedly surveyed the area over many years. In the second half of the 19th century, the Echmiadzin scholar Mesrop Smbatyants discovered two cuneiform inscriptions of Argishti I and Rusa III in the vicinity of Armavir. The first reconnaissance and survey excavations were organized in 1880 by A. D. Yeritsov and A. S. Uvarov [22].

Over different periods, the Armavir Archaeological Expedition was led by N.Ya. Marr, S.V. Ter-Avetisyan, S. Ter-Hakopyan, B.N. Arakelyan, A.A. Martirosyan, R.M. Torosyan, G.A. Tiratsyan, I.A. Karapetyan, and S.G. Hmayakyan. The Nor Armavir cemetery was excavated during the 2021 field season under the direction of S.G. Hmayakyan, and the burial analyzed in the present study dates to the 6th–5th centuries BC. The present study provides bioarchaeological data on an individual from this burial. The village of Nor Armavir is located to the northwest of the "Fortress of Saint David." More than 50 burials dating to the 8th–6th centuries BC were discovered and excavated within household plots in the village (**Fig. 1**), 17 of which were karas burials (interments in large ceramic vessels or pithoi) [13].

The bioarchaeological material from the Nor Armavir burial complex was excavated in Sector 3 ("Levon's Gardens") by the archaeological expedition of the Institute of Archaeology and Ethnography of the National Academy of Sciences of the Republic of Armenia, under the direction of S.G. Hmayakyan (archaeologists M.S. Hmayakyan and N.G. Tiratsyan). The article analyzes the skeletal remains from burial No. 6 of the Nor Armavir cemetery, which was excavated in 2021 (**Fig. 1**). This burial is unusual in that three individuals were interred in each layer, arranged one above the other. The skeleton from grave No. 6 were dated using relative (archaeological) methods. Other burials at the Nor Armavir cemetery exhibit comparable structural features, including grave type and skeletal positioning. The anthropological materials are curated in the Physical Anthropology Laboratory of the Institute of Archaeology and Ethnography, National Academy of Science, Republic of Armenia (Yerevan).

---

[1] 40°09′N 44°03′E

Fig. 1. Map of Armenia showing the location of Nor Armavir (drawing by A.Yu. Khudaverdyan), with the burial analyzed in this study shown at the top (drawing by S.G. Hmayakyan).

Detailed examination of the skeleton was conducted to evaluate preservation and completeness and to estimate the sex and age at death of the individual. Morphological characteristics of the pelvis and skull were used for sex determination [4, 28]. Age at death for the adult individual was estimated using a combination of pubic symphysis morphology [10, 15, 23], changes to the auricular surface [19], degree of epiphyseal fusion [4], dental wear [1], and cranial suture closure [23].

Diagenetic changes were evaluated macroscopically and through spectrometric analysis and were distinguished from pathological bone responses based on their distribution, structural organization, and relationship to the original cortical architecture.

A noninvasive X-ray study of human bone was conducted using experimental facilities for X-ray fluorescence (XRF) spectral analysis and microtomography (MicroCT) imaging at the Institute of Applied Problems of Physics (Yerevan, Armenia). XRF was employed to determine the elemental composition of the sample. Measurements were performed using a custom-designed setup comprising a BSV-25 X-ray tube and a silicon drift detector (AMPTEK-SDD). The X-ray beam was collimated using two narrow slits to achieve a beam size of 1 mm (vertical) × 0.1 mm (horizontal). XRF spectra were collected from four distinct points on the sample. The X-ray tube operated at 33 kV and 10 mA, with an exposure time of 300 seconds, kept constant across all measurements. Potential measurement errors inherent to the X-ray system were acknowledged and controlled by repeating measurements and maintaining consistent acquisition parameters across all samples.

Microtomographic imaging was carried out using a specialized system that included an XRB150PN6004009 X-ray source (Spellman High Voltage Electronics) and a Care View 750MT flat-panel detector (CareRay Digital Medical Technology). System control, data acquisition, and image reconstruction were managed using the T4 software platform, developed at Tomsk Polytechnic University (available at https://rsp.tpu.ru/tech/). This configuration enabled the capture of high-resolution X-ray images with a spatial resolution of approximately 60 μm. The X-ray tube operated at 70 kV and 1 mA, and the emitted beam was filtered through a 1 mm thick aluminum foil to optimize image contrast and reduce beam hardening effects.

Results

Skeleton 6 belonged to an adult male, aged approximately 40–45 years at the time of death. Sex was determined based on pelvic and cranial morphology. Age at death was estimated using a combination of changes to the auricular surface, degenerative bone conditions, dental wear, and cranial suture closure. Based on these features, the individual's age at death is estimated at 40–45 years. The skeleton is moderately well preserved, with most elements present; some bones exhibit post-mortem damage (**Fig. 2**).

The tibia shows marked enlargement involving the proximal metaphysis and the upper half of the diaphysis. A transverse section of the bone, resulting from post-mortem breakage, reveals pronounced cortical thickening and complete sclerotic obliteration of the medullary cavity by newly formed spongy bone. A large subcortical cavitation is present in the superolateral portion of the bone (**Fig. 3**). Plaque-like areas of new bone formation are observed on both the medial and lateral surfaces of the distal metaphysis. Bone sequestra and drainage channels (cloacae) are absent.

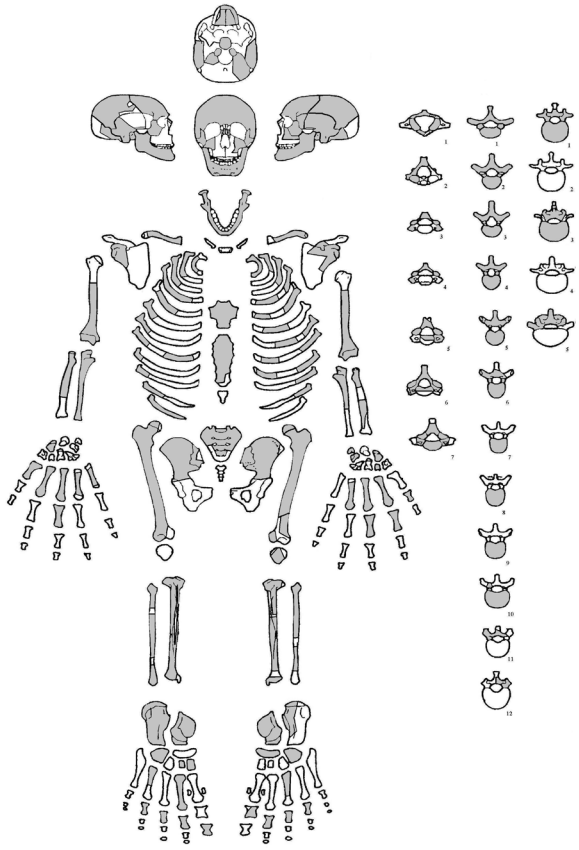

Fig. 2. Completeness of the human skeleton (grey colour – skeletal elements present, white – absent)

Radiographic examination demonstrates a thickened cortex in the diaphyseal region of the right tibia, accompanied by progressive narrowing of the medullary cavity. Computed tomography (CT) sections obtained at different levels provide clearer visualization of partial (**Fig. 4**) and complete obliteration of the medullary canal, as well as localized circumferential cortical thickening and the presence of bone lacunae. All bones were carefully cleaned prior to scanning, and the medullary cavities were free of soil or other extraneous material. The diaphysis exhibits a characteristic fusiform expansion. The narrowing of the medullary cavity is due to the formation of endosteal bone deposits along the inner cortical surface, reflecting a pathological response.

In some areas, against the background of cortical thickening and osteosclerosis, zones of osteodestruction are observed in the form of polymorphic, partially coalescing resorption cavities, producing a characteristic "moth-eaten" appearance of the dense bone tissue (**Figs. 4, 5**). The affected region exhibits increased radiodensity, consistent with osteosclerosis. Diagenetic changes were excluded by examining bone microstructure, evaluating the distribution of mineral deposits, and confirming that the cortical thickening followed anatomical patterns rather than irregular post-mortem mineralization.

Fig. 3. The cortical layer along the anterior medial surface of the tibia is thickened, areas of heterogeneous density are noted.

Multiple regions of the tibia are involved in the pathological process. Areas of bone necrosis (bone marrow infarction) were identified, resulting from insufficient blood supply and leading to the death of bone marrow and trabecular bone. This process contributed to narrowing and eventual obliteration of the medullary canal (**Fig. 3**). The fibula is unaffected and appears normal.

Computed tomography of the tibia revealed pronounced cortical thickening, narrowing, and obliteration of the medullary canal (**Fig. 5**). Extensive bone sclerosis is

clearly visible in both longitudinal and cross-sectional views, confirming pathological endosteal bone growth rather than taphonomic filling.

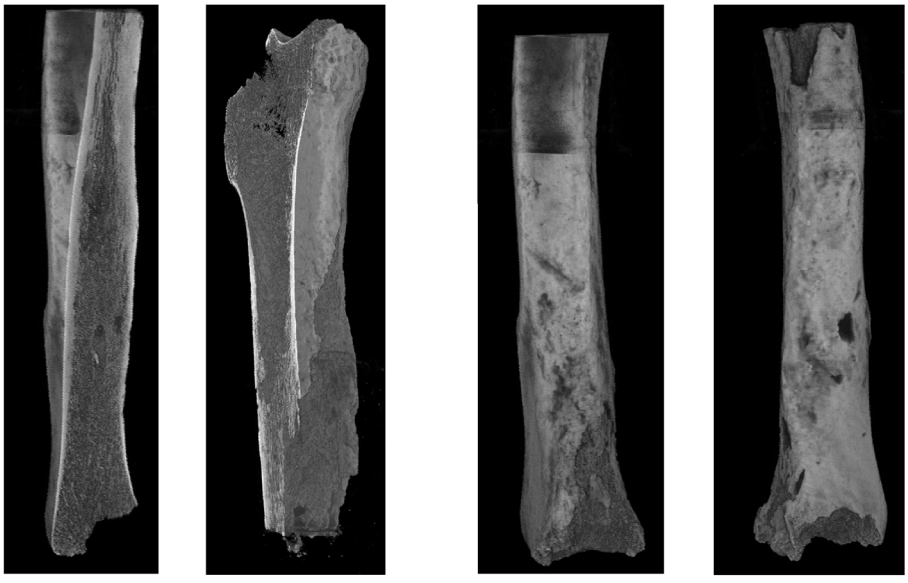

Fig. 4. On the surface of the tibia, areas of non-uniform density are observed, including ground glass opacity; a zone of bone marrow infarction is observed.

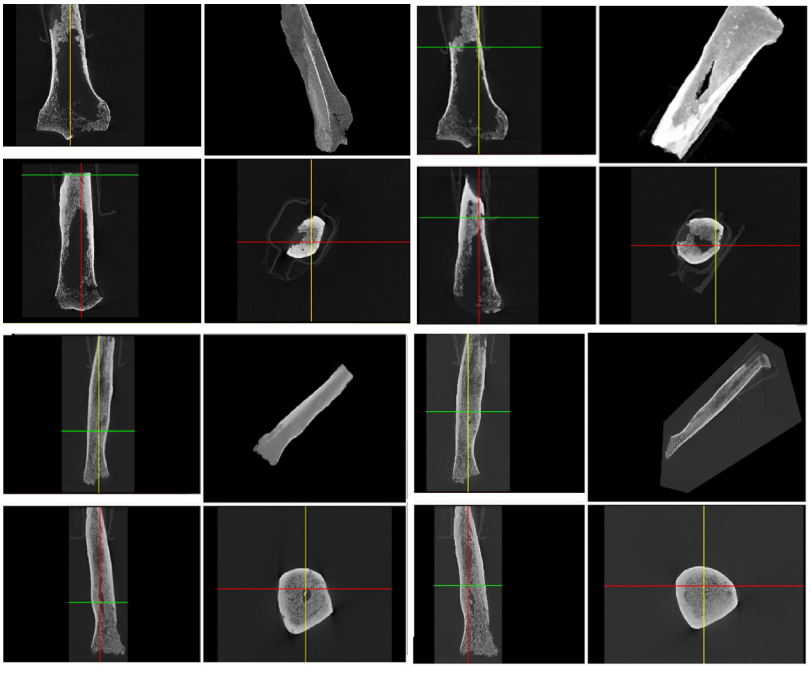

Fig. 5. X-ray fluorescence spectrometric analysis of several areas of the tibia.

Calcium (Ca) values in the tibia ranged from 77.662 % to 99.463 %, indicating post-mortem diagenetic alteration rather than the original biogenic composition of the bone **(Table 1)**. Similarly, strontium (Sr) concentrations likely reflect diagenetic uptake. Manganese (Mn) and iron (Fe) levels were relatively low, amounting to 2.056 µg/g and 13.171 µg/g, respectively. In contrast, the concentration of scandium (Sc) was notably elevated, reaching 12.839 µg/g. For comparison, the average scandium content in human skeletal bone is approximately 1–2 µg/kg, with a commonly cited mean value of about 1.5 µg/kg [5]. Given the unusual Sc enrichment, this observation may reflect unique environmental or pathological incorporation, and warrants further discussion.

Fig. 6. Dimensions of the tibia (upper transverse (1, 3: right 32,9 mm: 2, 44: left 32 mm), upper sagittal (1, 3: right 31 mm: 2, 44: left 21 mm); lower transverse (1, 3: right 31,5 mm: 2, 44: left 29 mm), upper sagittal (1, 3: right 33 mm: 2, 44: left 24 mm). Post-cranial skeleton without evidence of pathological changes (2, 4, 5-8).

No bone lesions or traumatic injuries were observed in the left tibia (**Fig. 6)**. Other elements of the cranial and post-cranial skeleton showed no additional evidence of pathological changes, including trauma.

Discussion

In the individual from Nor Armavir, several pathological features were documented – including pronounced cortical thickening in the anterior midshaft region of the tibia, narrowing and obliteration of the medullary canal, and extensive bone sclerosis. The medullary canal was thoroughly cleaned of soil and other debris prior to examination, and CT imaging confirmed that the cavity was filled with endosteal bone rather than post-mortem material, suggesting that the obliteration reflects a pathological process rather than taphonomic accumulation. This condition has been described in the literature under various terms, including chronic osteomyelitis with proliferative

periostitis and non-suppurative sclerosing osteomyelitis [25, 33, 34. 31]. In the present case, the pathological changes are predominantly endosteal, affecting the medullary cavity rather than the periosteal surface. The generally accepted term for this entity is Garré's sclerosing osteomyelitis.

Garré's osteomyelitis is classically characterized by fusiform enlargement of the affected bone, marked thickening and sclerosis of the cortical layer (dense compact bone), and narrowing or complete obliteration of the medullary canal. The differential diagnosis of Garré's osteomyelitis requires exclusion of other skeletal pathologies, including chronic suppurative osteomyelitis, fibrous dysplasia, malignant bone tumors (osteosarcoma, Ewing sarcoma), benign lesions (osteoid osteoma, eosinophilic granuloma, osteoblastoma), Paget's disease, as well as syphilitic bone disease [8, 11, 14, 18, 24].

Although Garré's osteomyelitis represents a form of chronic osteomyelitis, classic chronic osteomyelitis typically presents with foci of bone destruction, sequestra, and draining sinuses. In contrast, Garré's osteomyelitis is dominated by hyperostosis and sclerosis, rather than suppurative lesions. Fibrous dysplasia may show overlapping features with Garré's osteomyelitis; however, Garré's osteomyelitis is associated with a characteristic spiculated ("needle-like") periosteal reaction, whereas fibrous dysplasia more often exhibits a diffuse, "ground-glass" or hazy radiographic appearance. A similar sclerotic pattern may be observed in malignant bone tumors, such as osteosarcoma and Ewing sarcoma. Nevertheless, these neoplasms typically demonstrate more aggressive cortical destruction and permeative bone loss [6], features that are absent in Garré's osteomyelitis. Ewing sarcoma is also rare in individuals older than 30 years. Radiologically, it is characterized by an aggressive lytic lesion with a prominent periosteal reaction, often described as an "onion-skin" pattern. In the present case, the age at death, the absence of extensive cortical destruction, and preservation of the original diaphyseal architecture argue strongly against a diagnosis of Ewing sarcoma. In syphilitic bone disease, the pathological process is typically polyostotic, affecting multiple skeletal elements simultaneously. Deformation of the affected bones lacks the regular fusiform configuration characteristic of Garré's osteomyelitis, and the external contours are often irregular, undulating, or serrated, as seen in crest-like or circular periostitis. Although both syphilitic lesions and Garré's osteomyelitis are associated with hyperostosis and sclerosis, syphilis is usually accompanied by well-demarcated, rounded destructive foci of varying size, surrounded by sclerotic rims, corresponding to gummatous lesions – features not observed in the present case.

Benign bone lesions, such as osteoid osteoma and eosinophilic granuloma, typically display less extensive sclerosis or a more specific anatomical localization than that observed in Garré's osteomyelitis. Osteoblastoma, although classified as a benign tumor, is locally aggressive and shows a marked predominance in males (approximately 2:1), most frequently affecting adolescents and young adults, with the majority of cases reported between 10 and 25 years of age. The posterior elements of the vertebral column represent the most common site of involvement; long bones, particularly the femur and tibia, may also be affected, usually involving the medullary cavity and diaphysis, with

epiphyseal localization being rare. Osteoblastoma is characterized by a central lesion typically exceeding 2 cm in diameter and surrounded by a reactive sclerotic rim [2]. In the present case, the age of the individual falls outside the most commonly reported range for osteoblastoma. In addition, the affected bone segment is substantially larger, and the morphology and distribution of internal cavitations differ from those typically described for osteoblastoma, making this diagnosis unlikely.

Paget's disease of bone is a metabolic skeletal disease, characterized by excessive resorption followed by excessive formation of bone, with abnormal bone remodeling. A critical element in the differential diagnosis concerns the condition of the medullary cavity. Involvement is usually polyostotic and asymmetric, and the most affected bones are the pelvis, spine, skull, femur, and tibia. In Garré's osteomyelitis, progressive endosteal bone apposition commonly leads to marked narrowing or even complete obliteration of the medullary canal. Moreover, Paget's disease frequently involves overall bone expansion and polyostotic distribution, features that further distinguish it from the localized, obliterative sclerosis observed in Garré's osteomyelitis.

Taken together, the macroscopic, radiological, and differential diagnostic evidence - while acknowledging the presence of post-depositional diagenetic alterations - suggests that the tibial pathology may represent a form of Garré's sclerosing osteomyelitis.

The lesion is best understood as a long-standing, localized, non-suppurative inflammatory process dominated by excessive bone formation and sclerosis, features that cannot be adequately explained by diagenetic processes alone. Post-depositional diagenetic alterations are indeed present and are evident in both the macroscopic appearance of the specimen and the spectrometric data. The extremely high calcium (Ca) values recorded in the tibia (77.662–99.463%) markedly exceed the expected range for archaeological bone with preserved collagen (26–38%) [4]. Such elevated Ca concentrations clearly reflect advanced post-depositional diagenetic mineral alteration of the bone tissue. Accordingly, the spectrometric data are interpreted as evidence of diagenetic overprint rather than as a direct indicator of pathological bone metabolism. Similarly, strontium (Sr) concentrations likely reflect diagenetic uptake. Manganese (Mn) and iron (Fe) levels were relatively low.

Given the unusual Sc enrichment, this finding may reflect specific geochemical conditions of the burial environment or a pathological alteration in bone metabolism that facilitated the atypical incorporation of trace elements. Scandium is not typically reported in elevated concentrations in archaeological bone, and its biogenic role remains poorly understood. Therefore, the detected enrichment is unlikely to represent a random fluctuation and may instead indicate selective uptake or post-depositional chemical interaction under particular environmental conditions. At the same time, chronic inflammatory processes and sustained bone remodeling – such as those inferred in the present case - could potentially influence trace element distribution and retention within newly formed bone tissue. While scandium has been discussed in modern medical literature as potentially associated with sclerosing osteomyelitis [9, 12, 16], the evidence remains limited. Although the available data do not allow us to conclusively distinguish between diagenetic and biogenic pathways, the unusual Sc signal warrants further targeted geochemical and histological investigation.

Importantly, while diagenetic processes may modify bone surface texture and mineral composition, they do not adequately account for the extent, distribution, and organization of the excessive bone formation and sclerosis observed in the tibia. These features are therefore interpreted as primarily pathological in origin and consistent with Garré's sclerosing osteomyelitis rather than post-depositional alteration alone.

Importantly, no pathological alterations were observed in the contralateral (left) tibia or in other elements of the cranial and post-cranial skeleton. This localization of the pathological and elemental changes to a single bone favors a localized chronic process rather than a systemic metabolic disorder.

Cases of sclerosing osteomyelitis with morphology comparable to that described by Garré in modern clinical literature have been reported in ancient populations. Manchester [21] documented cases of chronic osteomyelitis with pronounced periosteal appositions on long bones but did not distinguish Garré's osteomyelitis as a separate entity. Ortner [27] noted that Garré's osteomyelitis may be misinterpreted as nonspecific chronic osteomyelitis with periosteal reaction. Similarly, Roberts & Manchester [30] described periosteal reactions and sclerotic processes without defining Garré's osteomyelitis as a distinct diagnostic category. Dutour et al. [7] reported cases of cortical thickening with periosteal apposition in ancient Egyptian skeletons; although these changes may correspond to Garré's osteomyelitis, no definitive identification was proposed.

Within the paleopathological literature, only two cases of Garré's sclerosing osteomyelitis - a chronic form of osteomyelitis characterized by intense periosteal reaction with minimal or absent suppuration - have been explicitly reported [11, 29]. One case involves a tibia recovered from an archaeological site in Poland and dated to the medieval period [29]. The other documents sclerosing osteomyelitis of the tibia from the medieval church cemetery of Monte di Croce in Tuscany, Italy [11].

Conclusions

1. The pathological changes observed in the tibia from Nor Armavir are characterized by pronounced cortical thickening, extensive sclerosis, and near-complete obliteration of the medullary canal due to endosteal bone formation.
2. Macroscopic and CT data demonstrate that the obliteration of the medullary cavity represents a true pathological process rather than post-mortem sediment infill or taphonomic alteration.
3. Differential diagnostic analysis excludes a wide range of alternative conditions, including chronic suppurative osteomyelitis, fibrous dysplasia, malignant and benign bone tumors, Paget's disease, and syphilitic bone involvement, based on the absence of characteristic destructive, polyostotic, or neoplastic features.
4. The combination of morphological and radiological features is most consistent with Garré's sclerosing osteomyelitis, a localized, chronic, non-suppurative inflammatory condition dominated by bone sclerosis and hyperostosis.

5. Spectrometric analysis indicates significant post-depositional diagenetic alteration, as reflected by elevated calcium and altered trace element composition; however, these changes do not account for the structural organization and extent of pathological bone formation.

6. The unusual enrichment in scandium may reflect either specific burial geochemistry or altered bone metabolism associated with chronic inflammation, although its origin remains unresolved and requires further investigation.

7. The restriction of pathological changes to a single bone element supports the interpretation of a localized process rather than a systemic metabolic disorder.

8. This case represents a rare example of Garré's sclerosing osteomyelitis in the paleopathological record and contributes to the limited number of securely identified cases reported in archaeological populations.

References

1. **AlQahtani, S. J., M. P. Hector, H. M. Liversidge.** Brief communication: the London atlas of human tooth development and eruption. - *American Journal of Biological Anthropology*, **142** (3), 2010, 481–490.
2. **Atesok, K. I., B. A. Alman, E. H. Schemitsch, A. Peyser, H. Mankin.** Osteoid osteoma and osteoblastoma. - *Journal of the American Academy of Orthopaedic Surgeons*, **19**, 2011, 678–689.
3. **Evaristo, B., M. Claudio, A. Tiziana.** Sclerosing osteomyelitis of Garré periostitis ossificans. - Journal of Craniofacial Surgery, **13** (6), 2002, 765–768.
4. Buikstra, J., D. D. Ubelaker. *Standards for the data collection from human Skeletal remains*, Fayetteville: Arkansas Archaeological Survey Research Series, 1994.
5. **Burton, J. H.** *Bone chemistry and trace element analysis*, in: Katzenberg M. A., Saunders, S. R. (eds.) Biological Anthropology of the Human Skeleton. Wiley-Liss, USA, 2008, pp. 443–460.
6. **de Moraes, F. B., M. T. Motta, A. A. Severin, D. de Alencar Faria, F. de Oliveira César, S. de Souza Carneiro**. Garré's sclerosing osteomyelitis: case report. - *Revista Brasileira de Ortopedia*, **49**, 2014, 401-404.
7. **Dorfman, H., B. Cerniak.** *Ewing Sarcoma and Related Entities*, Mosby, St Louis, 1998, pp. 607–642.
8. **Dutour, O., G. Pálfi, J. Bérato, J-P. Brun.** Paleopathology of the spine and ribs. In Diseases in Antiquity: A Survey of the Diseases, Injuries, and Surgery of Early Populations (Eds. D. E. Brothwell & A. T. Sandison), Springfield, IL: Charles C. Thomas, 1994, pp. 635–650.
9. **Fadil, M., A. Farouki, R. Saouab, H. En-Nouali, J. E. Fenni, Z. Toufga.** Garré's chronic sclerosing osteomyelitis: An overview of clinical and radiologic features. - *Oxford Medical Case Reports*, **12**, 2025, 1058-1061
10. **Gilbert, B. M., T. W. Mckern.** *A method for aging the female os pubis*. - American Journal of Physical Anthropology, **38**, 1973, 31-38.
11. **Giuffra, V., A. Vitiello, S. Giusiani, D. Caramella, G. Fornaciari.** A possible case of Garre's sclerosing osteomyelitis from Medieval Tuscany (11th–12th centuries). - International Journal of Paleopathology, **11**, 2015, 51–55.

12. **Ghazali, F. R., A. H. Z. Samsudin.** Sclerosing osteomyelitis of Garré: A Clinico radiological correlation. – *Cureus,* **14** (7), 2022, e26866.
13. **Hmayakyan, S. G., N. V. Tiratsyan, M. S. Hmayakyan.** Karasnoye and "clay box" burials from the 2016 excavations in Argishtikhinili. Preliminary report, in: On the other side of Aragats: archaeological research dedicated to the memory of Telemak Khachatryan. Yerevan, 2018, pp. 175–181. [in Armenian]
14. **Kashima, T. G., N. G. Gamage, U. Dirksen, C. L. Gibbons, S. J. Ostlere, N. A. Athanasou**. Localized Ewing sarcoma of the tibia. - **Clinical Sarcoma Research**, **3**, 2013, 2.
15. **Katz, D., J. M. Suchey.** Age determination of the maleos pubis. - American Journal of Physical Anthropology, **69**, 1986, 427-435.
16. **Khan, A. G. S., H. Ahsin, S. Khan, A. Rafique, R. Kamal.** Garre's osteomyelitis of long bone in adult. - *Journal of Ayub Medical College Abbottabad,* **36** (3), 2024, 674-677.
17. **Khorenatsi, M.** *Istoriya Armenii* / Per. N. O. Emina [*History of Armenia* / Translated by N. O. Emin], Moscow, 1893. [in Russian]
18. **Lee, C. H., S. H. Han, B. Y. Yoon, Y. W. Lee.** Monostotic Paget's disease of the tibia in Korea. - Clinical Rheumatology, **23**, 2004, 381–382.
19. **Lovejoy, C. O., R. S. Meindl, T. R. Pryzbeck, R. P. Mensforth.** Chronological metamorphosis of the auricular surface of the ilium: A new method for the determination of adult skeletal age at death. - American Journal of Physical Anthropology, **68**, 1985, 15-28.
20. **Macnicol, M. F., A. C. Watts.** Haematogenous osteomyelitis. - Surgery (Oxford), **23** (1), 2005, 25-30.
21. **Manchester, K.** *The archaeology of discase*. Bradford, 1983.
22. **Martirosyan, A. A.** Argishtikhinili. Arkheologicheskiye pamyatniki Armenii. Urartskiye pamyatniki [Argishtikhinili. Archaeological Monuments of Armenia. Urartian Monuments], Yerevan, 1974. [in Russian]
23. **Meindl, R. S., C. O. Lovejoy, R. P. Mensforth, L. D. Carlos.** Accuracy and direction of error in the sexing of the skeleton: Implications for paleodemography. - American Journal of Physical Anthropology, **68**, 1985, 79-85.
24. **Moraes, de F. B., T. M. Motta, A. A. Severin, D. de Alencar Faria, F. de Oliveira César, S. de Souza Carneiro**. Garré's scle rosing osteomyelitis: case report. - *Revista Brasileira de Ortopedia,* **49**, 2014, 401-404.
25. **Nasir, N., K. Aquilina, D. Q. Ryder, C. J. Marks, C. Keohane.** Garré's chronic diffuse sclerosing osteomyelitis of the sacrum: a rare condition mimicking malignancy. - *British Journal of Neurosurgery,* **20**, 2006, 415-419.
26. **Nikomarov, D., M. Zaidman, A. Katzman, Y. Keren, M. Eidelman.** New treatment option for sclerosing osteomyelitis of Garré. - *Journal of Pediatric Orthopaedics B*, **22**, 2013, 577-582.
27. **Ortner, D. J.** *Identification of pathological conditions in human skeletal remains.* Academic Press, 2003.
28. **Phenice, T. W.** A newly developed visual method of sexing the os pubis. - *American Journal of Physical Anthropology*, **30**, 1969, 297-302.
29. **Prejzner, W., J. J. Gladykowska-Rzeczycka.** An attempt to evaluate the criteria for diagnosing nonspecifica inflammatory diseases observed on ancient skeletons. - *Przeglad Antropologiczny*, **60**, 1997, 103–109.
30. **Roberts, C., K. Manchester.** *The archaeology of disease.* Cornell University Press, 2007.

31. **Silva, A. J. S. G., J. A. Correia, F. Salvado, J. C. Romeu.** Garrè's Osteomyelitis regarding a clinical case and literature review: Garrè's Osteomyelitis a review. - European Journal of Stomatology, Oral and Facial Surgery, **2** (1), 2025, 02:01.
32. **Song, S., H. J. Jeong, H. K. Shin, E. Kim, S. J. Park, J. H. Park.** Sclerosing osteomyelitis of Garré: A confusing clinical diagnosis. - *Journal of Orthopaedic Surgery (Hong Kong)*, **27**, 2019, 2309499019874704
33. **Suma, R., C. Vinay, M. C. Shashikanth, V. V. Subba Reddy**. Garré's sclerosing osteomyelitis. - *Journal of Indian Society of Pedodontics and Preventive Dentistry,* **1**, 2007, 30-33.
34. **Vannet, N. B., H. L. Williams, B. Healy, R. Morgan-Jones.** Sclerosing osteomyelitis of Garré: management of femoral pain by intramedullary nailing. - *BMJ Case Reports* 2014: 10.1136/bcr-2014-206533.
35. **Volodina, V. D., A. A. Babkova, N. S. Serova, D. S. Bobrov, V. V. Zuev.** Garre's sclerosing osteomyelitis. – *Russian Electronic Journal of Radiology*, **12** (4), 2022, 153-158.

Table 1. X-ray fluorescence spectrometry analysis of several sections of the tibia (Figure 5)

Elt	Line	Intensity	Conc.
Precinct 1			
Ar	Ka	0.01	0.162
K	Ka	0.09	0.832
Ca	Ka	9.92	77.662
Ti	Ka	0.14	1.395
Mn	Ka	0.53	2.056
Fe	Ka	4.35	13.171
Sr	Ka	1.61	1.786
Nb	Ka	0.99	2.935
Tb	La	0.00	0.000
Total:			100.000
Precinct 2			
P	Ka	0.00	0.356
Ar	Ka	0.00	0.000
K	Ka	0.03	0.243
Ca	Ka	10.79	99.401
Mn	Ka	0.00	0.000
Fe	Ka	0.00	0.000
Sr	Ka	0.00	0.000
Zr	Ka	0.00	0.000
Nb	Ka	0.00	0.000
Tb	La	0.00	0.000
Total:	100.000		
Precinct 3			
P	Ka	0.00	0.000
Ar	Ka	0.00	0.000

Ca	Ka	9.45	87.051
Sc	Ka	0.54	12.839
Mn	Ka	0.00	0.000
Fe	Ka	0.00	0.000
Cu	Ka	0.00	0.000
Sr	Ka	0.08	0.110
Y	Ka	0.00	0.000
Nb	Ka	0.99	2.935
Tb	La	0.00	0.000
Total:	100.000		
Precinct 4			
Ar	Ka	0.00	0.000
Ca	Ka	21.18	99.463
Ti	Ka	0.03	0.221
Mn	Ka	0.00	0.000
Fe	Ka	0.00	0.000
Sr	Ka	0.45	0.316
Total:	100.000		